

Striatal origin of the pathologic beta oscillations in Parkinson's disease

M. M. McCarthy^{a,1}, C. Moore-Kochlacs^{a,2}, X. Gu^{b,2}, E. S. Boyden^c, X. Han^b, and N. Kopell^{a,1}

^aDepartment of Mathematics and Statistics, Boston University, Boston, MA 02215; ^bDepartment of Biomedical Engineering, Photonics Center, Boston University, Boston, MA 02215; and ^cMedia Lab, Massachusetts Institute of Technology, Cambridge, MA 02139

Contributed by N. Kopell, May 17, 2011 (sent for review December 28, 2010)

Enhanced oscillations at beta frequencies (8–30 Hz) are a signature neural dynamic pathology in the basal ganglia and cortex of Parkinson's disease patients. The mechanisms underlying these pathological beta oscillations remain elusive. Here, using mathematical models, we find that robust beta oscillations can emerge from inhibitory interactions between striatal medium spiny neurons. The interaction of the synaptic GABA_A currents and the intrinsic membrane M-current promotes population oscillations in the beta frequency range. Increased levels of cholinergic drive, a condition relevant to the parkinsonian striatum, lead to enhanced beta oscillations in the striatal model. We show experimentally that direct infusion of the cholinergic agonist carbachol into the striatum, but not into the neighboring cortex, of the awake, normal rodent induces prominent beta frequency oscillations in the local field potential. These results provide evidence for amplification of normal striatal network dynamics as a mechanism responsible for the enhanced beta frequency oscillations in Parkinson's disease.

computational model | acetylcholine | muscarinic | mouse

Enhanced beta frequency oscillations are correlated with bradykinesia, a disabling movement abnormality in Parkinson's disease patients (1). Improvement of bradykinesia correlates with a decrease in the enhanced beta frequency oscillations in the subthalamic nucleus (STN) and cortex of Parkinson's disease patients (2). However, the function of the beta oscillations in parkinsonian pathology remains elusive, and the source of these oscillations is unknown. Two predominating theories exist about the origin of these enhanced beta rhythms. One hypothesis proposes that oscillations arise from the interaction of the STN and the external segment of the globus pallidus (GPe); this is known as the STN/GPe pacemaker hypothesis (3). Evidence for the STN/GPe pacemaker hypothesis comes from a study showing that GPe and STN are able to generate synchronized oscillatory bursting activity in the range of 0.4–1.8 Hz in organotypic cultures of cortex-striatum-STN-GPe (4). A second theory of beta generation in Parkinson's disease entails cortical patterning of the STN (3). This theory derives partly from studies on anesthetized rats showing that, with dopamine depletion, oscillatory spiking activity in STN and GPe is correlated with and largely dependent on cortical slow-wave (~1 Hz) activity (5). For the cortical patterning, but not the STN/GPe hypothesis, there is experimental evidence for intrinsic production of the beta rhythm (6).

Degeneration of dopaminergic neurons that project to the striatum is a hallmark of Parkinson's disease pathology (7), but the striatum has been largely ignored as a possible source of beta frequency rhythms in Parkinson's disease. There are several reasons for ignoring the striatum. The striatum consists of an almost entirely inhibitory network of cells (99.7% are GABAergic and 0.3% are cholinergic in the rat neostriatum) (8). Furthermore, the predominant striatal cell type, the medium spiny neuron (MSN), rarely spikes (average rate of 1.1 ± 0.18 Hz in freely moving rats) (9). It is not evident that this largely inactive and inhibitory network can generate any independent activity, much less rhythmic activity at a relatively high frequency (8–30 Hz). However, mathematical modeling informs us that inhibition can create neuronal excitation

under certain conditions. Specifically, the activation or inactivation of slow currents can lead to the phenomenon of postinhibitory rebound spiking. Moreover, inhibitory networks of such neurons can produce rhythmic activity (10, 11). The frequency of the rhythm largely depends on the time constant of the slow current. At least one slow current is known to have a time constant of decay that allows postinhibitory rebound spiking to occur with a lag appropriate for the formation of beta frequency spiking: the M-current (10). The M-current is a noninactivating potassium current, and GABA_A inhibition can temporarily reduce this current, leaving the neuronal membrane in a more excited state (12). The MSNs of the striatum have an M-current and receive inhibition from each other through GABA_A synapses. Therefore, the MSNs of the striatum contain both the cellular and the network properties to support the generation of beta frequency oscillations.

We construct mathematical models of networks of MSNs and find that such networks are capable of generating robust beta oscillations. Perturbations that enhance the interaction between MSN M-current and GABA_A current increase the power of the population beta rhythm. An interesting prediction is that increases in either MSN background excitation (I_{app}) or MSN GABAergic inhibition will increase the power of beta oscillations in the model MSN network. Because increasing MSN excitation necessarily increases MSN to MSN inhibition, these seemingly opposite effects, in fact, work synergistically to create beta frequency oscillations in our model MSN networks.

Striatopallidal MSNs have high levels of dopamine D2 receptors and increase their excitability in response to loss of dopamine (13). Furthermore, loss of dopamine has been shown to increase beta oscillations in striatum (14). This finding is consistent with our model results, which predict enhanced beta oscillations in the subnetwork of striatopallidal MSNs after loss of striatal dopamine. MSN excitability can also be increased by other neuromodulators, most notably by the action of acetylcholine (ACh) on M1 receptors (13). This is important in the context of Parkinson's disease, because dopamine modulates ACh levels. Dopamine tonically inhibits ACh release in the striatum under normal physiological conditions by its action on D2 receptors (15). Moreover, antagonists of either D1 or D2 receptors as well as loss of striatal dopamine in the 6-hydroxydopamine (6-OHDA) rat, an animal model of Parkinson's disease, result in increased striatal levels of ACh (16).

As a first test of our model, we inject the muscarinic acetylcholine receptor agonist carbachol into the striatum of normal awake mice. As predicted, cholinergic agonists in the striatum induce enhanced beta frequency oscillations in the striatal local field potential (LFP). Neither striatal nor cortical LFPs show

Author contributions: M.M., E.S.B., X.H., and N.K. designed research; M.M., C.M.-K., X.G., and X.H. performed research; M.M., C.M.-K., X.G., and X.H. analyzed data; and M.M., E.S.B., X.H., and N.K. wrote the paper.

The authors declare no conflict of interest.

¹To whom correspondence may be addressed. E-mail: mmccart@bu.edu or nk@bu.edu.

²C.M.-K. and X.G. contributed equally to this work.

This article contains supporting information online at www.pnas.org/lookup/suppl/doi:10.1073/pnas.1107748108/-DCSupplemental.

increased beta oscillations after infusion of carbachol into the cortex, showing that striatal LFP beta is not the result of diffusion of carbachol into the neighboring cortex. Our combined computational and experimental results suggest that increased MSN excitation, which produces increased MSN to MSN inhibitory interactions, is a potential source of the enhanced beta rhythms in Parkinson's disease. Our modeling results also suggest that loss of dopamine and increased striatal ACh work in parallel to amplify beta oscillations in striatal networks in Parkinson's disease.

Results from Mathematical Models of Normal and Parkinsonian Networks of MSNs

Networks of MSNs Alone Produce Beta Oscillations. A raster plot of our 100-neuron striatal model (see *Computational Methods*) us-

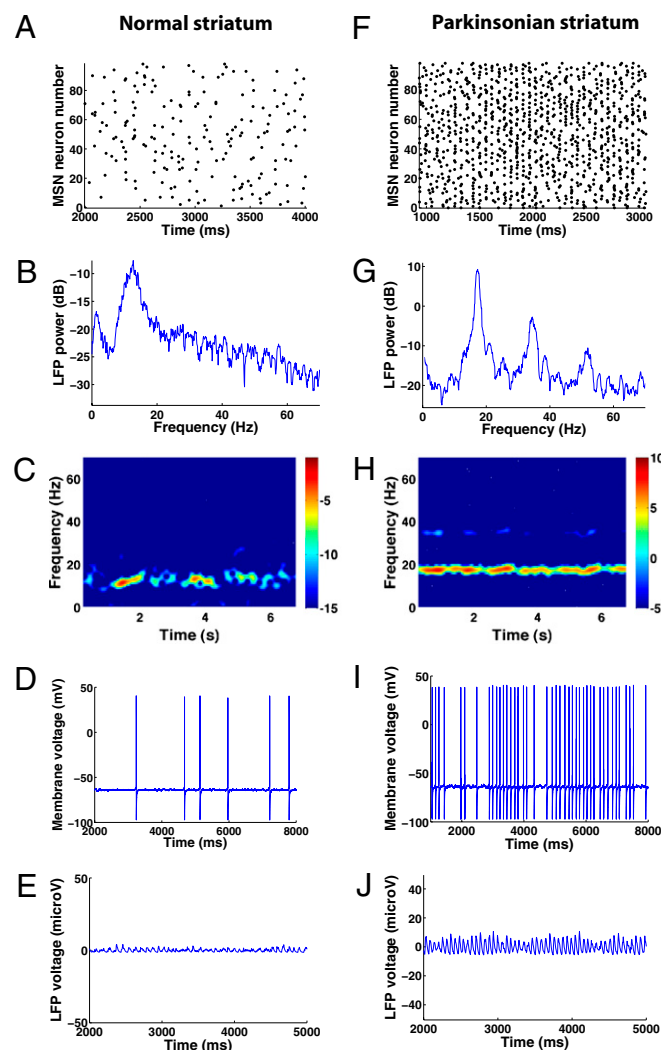


Fig. 1. Beta oscillations emerge in the model striatum under normal conditions and become enhanced under parkinsonian conditions. *A–E* are taken from the same 7-s simulation under normal conditions, and *F–J* are from the same 7-s simulation under parkinsonian conditions. (*A*) Raster plot of 100 reciprocally connected medium spiking neurons (MSNs) under normal, non-parkinsonian conditions. (*B*) Power spectral density of the model LFP. (*C*) Spectrogram of the model LFP. (*D*) Membrane voltage fluctuations from one MSN in the network. (*E*) Waxing and waning of the model LFP trace under normal conditions. (*F*) Raster plot of 100 reciprocally connected MSNs under parkinsonian conditions. (*G*) Power spectral density of the model LFP. (*H*) Spectrogram of the model LFP. (*I*) Membrane voltage fluctuations from one MSN in the parkinsonian network. (*J*) The model LFP trace under parkinsonian conditions.

ing weak all-to-all connections displays no readily observable pattern of activity among MSNs (Fig. 1*A*). However, analysis of the model LFP reveals a distinct peak in the low beta frequency range centered around 12.1 ± 0.7 Hz (Fig. 1*B*). The beta frequency oscillations wax and wane over time (Fig. 1*C*). The spiking of individual MSNs is irregular (Fig. 1*D*). The average spiking rate of the neurons in this network is 0.96 ± 0.03 Hz, consistent with the low average MSN spiking rate in vivo (9). The trace of the model LFP also contains waxing and waning beta frequency oscillations (Fig. 1*E*).

Beta Power and MSN Spiking Frequency Increase in Parkinson's Disease Model Striatum.

We simulate the loss of dopamine in the parkinsonian striatum indirectly through ACh-induced reduction of the M-current (see *Computational Methods*). Decreasing the maximal M-current conductance by 7.7% has pronounced effects on the striatal network dynamics [the percent decrease of the maximal M-current conductance (\bar{g}_m) depends on various parameters; for example, Fig. S1 shows a qualitatively similar model in which the M-current changes 41.2% between the normal and parkinsonian states]. MSN spiking becomes more obviously patterned into a beta frequency population rhythm (Fig. 1*F*). The LFP power peaks at a higher frequency (17.1 ± 0.32 Hz), and the peak power is higher than in the non-parkinsonian condition (Fig. 1*G*). This beta oscillation is persistent in contrast to the waxing and waning of the oscillation in the non-parkinsonian condition (Fig. 1*H*). Individual MSNs show more prominent subthreshold beta frequency oscillations because of the increased number of MSNs participating in the population beta rhythm, which provides individual MSNs with increased beta frequency synaptic input (Fig. 1*I*). MSNs spike more frequently than in the non-parkinsonian condition, with an average spiking rate of 4.9 ± 0.15 Hz. The animal literature is unclear; some studies show an increase in striatal activity with parkinsonism (9, 17), whereas others show a decrease (18). The model LFP contains a more pronounced and persistent oscillatory component in the beta frequency range (Fig. 1*J*). We note that the exact frequency range of oscillations found experimentally within the basal ganglia differs among papers; some describe 15–30 Hz oscillations, whereas others extend this range down to 8 Hz (19, 20).

Properties of the Mathematical Model

GABA_A-Current and M-Current Conductance Strengths and Background Excitation (I_{app}) Modulate LFP Beta Power and Peak Beta Frequency. Here, we are not looking at normal and parkinsonian states but merely at the change in beta as we change a parameter. The power and frequency of the beta oscillation tend to change nonmonotonically as the GABA_A conductance is increased. (Fig. S2 and Fig. S3*A* and *B*). Decreasing the M-current conductance or increasing I_{app} tends to increase both the power and frequency of the beta oscillation (Fig. S3*C–F*). In the absence of M-current, the MSN neurons resemble fast-spiking (FS) interneurons. We find that it is possible to obtain beta oscillations in networks of striatal FS interneurons alone but not in a regime supported by the experimental literature (Fig. S4).

Model Results Are Largely Invariant to Changes in Network Connectivity, Network Size, and Heterogeneity. Model striatal networks with either nearest neighbor connections or random network connections give qualitatively similar results to the network with all-to-all connections (*SI Note 4: Model results are largely invariant to changes in network connectivity, network size, and heterogeneity*; Fig. S5*A*). Increasing the number of MSNs to 400 or introducing heterogeneity by giving individual MSNs different maximal GABA_A conductances leads to qualitatively similar behavior to the networks with 100 MSNs and homogeneous maximal GABA_A conductances. Heterogeneity also helps us distinguish between the models of MSNs with and without M-current, because

MSNs without M-current are not robust to heterogeneity. Additional information is in *SI Note 4: Model results are largely invariant to changes in network connectivity, network size, and heterogeneity; Fig. S5B and Fig. S6.*

Experimental Results

Increase in Striatal Cholinergic Activity Leads to Increase in Striatal Beta Frequency Oscillations. We tested our model experimentally by recording the striatal LFP while infusing the cholinergic agonist carbachol into the striatum of normal awake, head-fixed mice. Carbachol (0.5–1 mM and 1–2 μ L) infusion directly into the dorsolateral striatum (stereotactic coordinate: AP (anterior posterior) = -0.2 to 0.8 , ML (medial lateral) = 2.0 – 2.5 , and DV (dorsal ventral) = 3.0 – 3.5) induced prominent beta frequency oscillations in simultaneously recorded LFP (Fig. 2*A–E*). Often, the observed increase in beta power was preceded with a brief decrease in beta power (Fig. 2*A*). Episodes of prominent increase in beta oscillations often last several hundred milliseconds to several seconds, and they often presented a slight decrease in frequencies from high to low beta during each episode (Fig. 2*D* and *E*). Upon striatal carbachol infusion, a tremor-like movement was observed on the contralateral side. We refer to this movement as tremor-like to indicate that the movement has a rhythmic component. We do not assume that these movements represent the parkinsonian tremor, which occurs at a higher frequency. These tremor-like movements often interrupt the enhanced beta oscillation episodes before each movement onset. This observation is consistent with evidence that desynchronization of beta frequency oscillations occurs in both non-Parkinson's and Parkinson's disease patients before movement, although the latency to premovement desynchronization is delayed in Parkinson's disease patients in the absence of L-dopa (21–23).

Of the six mice tested, it took 442 ± 119 ms (mean \pm SD) for beta power to increase after infusion onset. Because the infusion site is typically positioned 300–700 μ m away from the recording electrode, diffusion of carbachol from the infusion site to the recording electrode may account for a significant portion of this observed delay. After the increase in beta power, beta power often dropped below the baseline and stayed low for an extended period even at the end of the recording session, typically 1 h after the end of infusion (Fig. 2*F*).

To eliminate the possibility that the observed LFP change was caused by the pressure induced by drug infusion, which may activate mechano-sensitive mechanisms in the striatum, we infused carbachol at a lower concentration (0.1–0.2 mM, $n = 5$; three mice infused with 1–2 μ L and two mice infused with 4–5 μ L). Infusion of low-concentration carbachol failed to induce any change in the LFP, even with up to 5 μ L infusion. Beta power remained stable throughout the entire infusion period (Fig. 2*G*). Furthermore, we did not observe any reduction in beta power at the end of these recording sessions. Thus, the reduction in beta oscillations following augmentation as induced with high-concentration carbachol infusion cannot be explained by prolonged recording, confirming that the observed beta power reduction following beta increase is due to neural network mechanisms (Fig. 2*F*). In addition, in mice infused with low-concentration carbachol, no prominent tremor-like movement was observed.

Striatum Contains Sufficient Neural Network Components to Initiate Enhanced Beta Oscillations upon Cholinergic Activation. To examine whether the observed increase in beta oscillations is initiated in the striatum but not due to the diffusion of carbachol into the adjacent cortical regions, we infused carbachol (1 mM) into the cortex directly above the dorsolateral striatum where the striatal

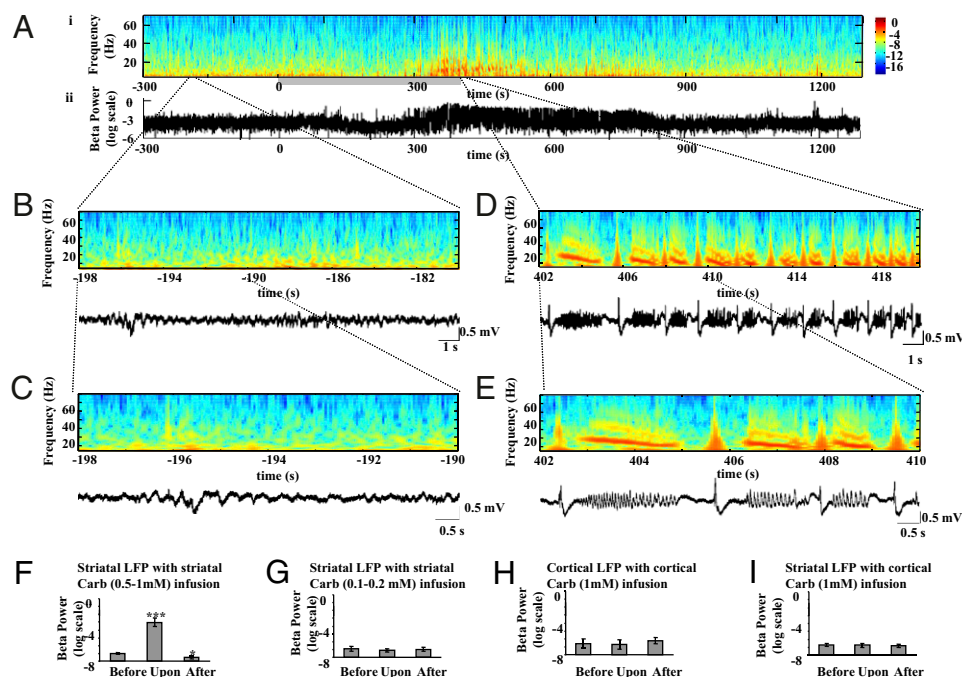


Fig. 2. Enhanced beta oscillations emerge in striatal LFP after carbachol infusion. (A) Power spectrum of the LFP recorded in the striatum of an awake, head-fixed mouse before, during, and after striatal carbachol infusion. (Upper) LFP power spectrum at 3–70 Hz on a log scale. (Lower) LFP power at beta frequency (10–30 Hz). (B and C) Power spectrum and LFP during a representative time window before carbachol infusion. (Upper) Power spectrum. (Lower) Corresponding LFP recorded in the striatum. (D and E) Power spectrum and LFP during a representative time window upon carbachol infusion. (Upper) Power spectrum. (Lower) Corresponding LFP recorded in the striatum. (F) Beta frequency power of the LFP recorded in the striatum before, during, and after carbachol (0.5–1.0 mM) infusion in the striatum ($n = 6$ mice; $***P < 0.005$ and $*P < 0.05$ paired t test compared to the power before carbachol infusion). (G) Beta frequency power of LFP recorded in the striatum before, during, and after low concentration carbachol (0.1–0.2 mM) infusion in the striatum ($n = 5$ mice). (H) Beta frequency power of LFP recorded in the cortex before, during, and after carbachol (1 mM) infusion in the cortex ($n = 5$ mice). (I) Beta frequency power of LFP recorded in the striatum before, during, and after carbachol (1 mM) infusion in the cortex ($n = 5$ mice).

infusion sites were located. We did not observe any increase in beta oscillations either locally in the cortex adjacent to the cortical infusion site or in the striatum directly below (Fig. 2 *H* and *I*). When advancing the infusion apparatus into the dorsolateral striatum and infusing carbachol (1 mM) in the striatal sites, we reliably induced an increase in beta oscillations in the striatum, confirming that the lack of beta increase on infusion in the cortical areas is due to the local network properties at the cortical infusion sites. These results demonstrate that carbachol diffusion into the cortical regions cannot explain the increase in striatal beta oscillations upon striatal infusion, thus suggesting that striatum is sufficient to induce enhanced beta oscillations.

Discussion

Our results indicate that the interaction between the MSN GABA_A current and the M-current generates beta frequency oscillations within striatal networks of MSNs. Increased MSN excitation promotes additional cellular-level interaction between these two currents, resulting in increased beta frequency power in the model LFP. Our experimental work verifies that increasing MSN excitability through amplification of striatal cholinergic tone, a condition relevant to Parkinson's disease, is sufficient to engender robust beta frequency rhythms in the striatum.

Although it is not surprising that a muscarinic agonist may increase MSN spiking rate (13), it is surprising that a muscarinic agonist can induce rhythmic activity in the beta frequency range in striatum. Our mathematical model of striatum predicts that the M-current plays an important role in establishing the beta frequency of the rhythm. The mechanism by which reciprocally connected GABAergic neurons with an M-current generate beta frequency population spiking is described in McCarthy et al. (10). The GABA_A current reduces the M-current by bringing the membrane potential closer to the potassium reversal potential. Reduction of the M-current depolarizes the neuron, potentially allowing the neuron to rebound spike. The dynamical interaction involving the slow time constants of decay of each current allows rebound spiking to occur with lags appropriate to the formation of a beta rhythm. An unintuitive consequence of this interaction is that increasing the GABA_A conductance can cause a greater reduction of the M-current and provide additional membrane excitation. As a result of increasing GABA_A conductance, the neuron may be able to rebound spike in situations that otherwise it would not, thus allowing greater participation of neurons in the network behavior. This mechanism of GABA_A potentiation-induced increase in membrane excitation is explained in more detail in Fig. S7. The production of beta rhythms in the context of low individual neuronal spiking rates and noise is discussed in *SI Note 6: Noise*. The mechanism of striatal beta rhythm production that we propose is dependent on the reversal potential of GABA_A being low (around -80 mV) such that the GABA_A reversal potential is close enough to the potassium reversal potential to cause suppression of the M-current when GABA_A is activated. This is supported by findings of the MSN inhibitory postsynaptic current reversal potential around -76 mV (24), although other studies report a more positive reversal potential (-62 and -64 mV) (25, 26) (see *SI Note 7: Reversal Potentials*). Our study suggests that the striatum contains the necessary neural network components to augment beta oscillations upon excitation of MSNs and that network interactions between MSNs alone, independent of striatal GABAergic interneurons, may be capable of creating beta frequency oscillations. Furthermore, the ability of our model to produce beta and to increase that beta in the parkinsonian state are both largely invariant to the pattern of network connectivity. This is an important result, suggesting that the beta rhythms in striatum may be quite robust to plastic changes in network connectivity.

Because MSN to MSN connections are very weak, their function in the striatal network is unclear (24). Our results here suggest that these weak connections structure the spiking of MSNs so

that the latter is more likely to spike at the same phase of the beta cycle. Furthermore, any modulator of the GABA_A current will influence the magnitude and peak frequency of the MSN network beta oscillation. Increasing the GABA_A conductance increases the peak frequency of the beta oscillation. Because elevated MSN spiking rates increase MSN to MSN GABAergic inhibition, any potentiator of MSN excitability increases the beta frequency oscillation in our model MSN network. Thus, the weak GABA_A synapses between MSNs generate a highly modulable system in which both the power and the frequency of the beta oscillations are regulated by modulators of either MSN excitability or the GABA_A current. Although the functional physiological significance of both normal and pathological beta rhythms remains to be elucidated, a high degree of modulation provides this system with the flexibility to adapt to a range of behavioral conditions. Additional study of this system will reveal the extent to which modulators of GABA_A and the M-current can create beta rhythms in the MSN (*SI Note 8: Other currents in MSNs* has more discussion of this topic).

Our models predict increased MSN spiking in the parkinsonian state. Such increased spiking activity of MSNs has been reported in animal models of Parkinson's disease (9, 27). Our models also predict an increased number of MSNs spiking at the same phase of each cycle of the beta rhythm under parkinsonian conditions. Because MSNs are the only output neurons of the striatum, increasing the number of synchronously spiking MSNs at each cycle of the beta oscillation has important implications concerning the transmission of this rhythmicity to downstream structures. Substantial convergence of input is thought to occur between the striatum and the globus pallidus (GP) because of the much larger number of neurons in striatum compared with the GP (28). Thus, increasing MSN synchrony should lead to stronger GABAergic input onto GP neurons. Because GP neurons can phase reset in response to GABA_A inhibitory input (29) and in particular, to transient striatal input (30), the GP neurons receiving the synchronous MSN input may be patterned into the beta frequency oscillation. Additionally, in Parkinson's disease, D1 and D2 MSNs are thought to decrease and increase their excitability, respectively, in response to loss of dopamine (13, 31). Our model predicts the power of the beta oscillation scales with the level of excitation in the MSN population. Thus, we expect the population of D2 MSNs to increase network beta in the parkinsonian state and the population of D1 MSNs to decrease network beta in the parkinsonian state. Furthermore, because the rate of unilateral connectivity from D1 to D2 MSNs is relatively low (6%) (32), we do not expect significant interaction between these populations. Thus, we expect the mechanism of beta rhythm production that we describe here to be most applicable to the dynamics of neurons that project mainly to GPe (D2 MSNs) in the context of Parkinson's disease. This is in line with current thinking that suggests that the direct pathway is underactive in Parkinson's disease and that the indirect pathway is overactive (1).

Our computational model producing striatal beta oscillations is independent of both specific external input and input from intrastriatal FS interneurons. In fact, we expect that striatal FS interneuron input may be diminished in Parkinson's disease and in our experiments with carbachol, because ACh attenuates FS inhibition of MSNs through presynaptic muscarinic receptors (33). Thus, adding FS interneurons to the model will only affect the results of the normal, non-parkinsonian case. Because we are not trying to replicate all of the LFP patterns of the normal striatum but rather, explain the parkinsonian beta oscillation, we feel that a more complex model of the striatum with FS cells is not necessary. Similarly, we expect glutamatergic input from cortex and thalamus to be reduced, because activation of striatal M1 muscarinic receptors decreases both the probability of glutamate release from presynaptic terminals as well as the potency

of individual glutamatergic synapses onto MSNs (34). However, we expect striatal levels of ACh, which are thought to come mainly from striatal cholinergic interneurons, to be elevated in Parkinson's disease (15, 16). We note that anticholinergics were the only available pharmacologic treatment for Parkinson's disease until the introduction of L-dopa in the 1960s (35). Our model predicts that some of their efficacy may reside in their ability to decrease striatal beta oscillations.

The experimental results show additional changes not predicted by the computational models. The model does not predict the lower delta and theta frequency rhythms seen in the absence of carbachol. This may be due to the presence of other striatal cell types such as FS neurons not present in our model. Tremor-like activity is not a prediction of our model; beta oscillations in Parkinson's disease do not necessarily correlate with tremor (2). Even in the present study, however, the tremor can be viewed as interrupting the beta oscillation. The mouse beta oscillations are interrupted by periods of decreased beta before and after the tremor movement. We attribute this to some in vivo compensatory change in the response to increased beta in the striatum, possibly modulated by thalamic input, as there is evidence that parkinsonian tremor is modulated by the thalamus (36). Also, in the mice, there is a drifting in the frequency of beta, which attains its highest values postmovement, drifts to lower values, and disappears before the tremor movement. Our model provides several potential explanations for frequency drift, including changes to the GABA_A or M-current conductances or changes in the background excitation. However, it is unclear which of these mechanisms might be contributing to the frequency drift in the mouse striatum. We also cannot account for the decreases in beta seen before the carbachol-induced rise in beta, which might represent a homeostatic response to the carbachol infusion. However, the decrease in beta that follows the rise in beta may be due to overrecovery of the M-current, in which increases in the M-current follow its suppression (37). Differences between our study and other published studies as well as other models of striatal MSNs are discussed in *SI Note 9: Other Related Studies*.

Other studies suggest that the enhanced beta rhythms in Parkinson's disease may arise from the interaction of the STN and the GPe or from the cortical patterning of STN (3). Both theories were developed initially from experimental studies showing very low frequency oscillations (less than 1.8 Hz) developing in structures relevant to Parkinson's disease (4, 5). In contrast, our studies on striatum show the emergence of robust beta frequency oscillations in both our computational and experimental results. Computational models of the STN-GPe network show that, under certain conditions, the system exhibits rhythmic oscillations within the frequency range appropriate to Parkinson's disease (3, 38). Interestingly, the critical condition for this to occur is increased inhibitory input from the striatum; increased patterned inhibitory input is a prediction of our model. Furthermore, the failure of cortical infusions of carbachol to induce beta oscillations is evidence against the idea that increasing gain anywhere within the cortico-basal ganglia-thalamic loop is sufficient to produce beta oscillations. Additionally, most of the mechanisms of beta production that we are currently aware of in the cortex are completely different from the mechanism of beta rhythm generation that we describe in our striatal model, and depend on excitatory cells (39, 40). One study using rat brain slices shows that high beta can be elicited from M1 by coapplication of carbachol and kainate (6). This beta rhythm appears to be dependent on networks of GABAergic interneurons as well as on excitatory cell drive similar to our model of striatum. However, Yamawaki et al. (6) think the mechanism of beta in M1 is similar to the mechanism producing persistent gamma oscillations in other cortical areas.

The results presented here highlight the powerful combination of mathematical and experimental approaches in addressing problems in systems neuroscience. Dynamics of biological systems do not readily yield to direct observation using even the most sophisticated experimental approaches. We show here that informed biophysical modeling can be highly predictive of complex biological dynamics. Additionally, these findings also have broad implications in understanding beta oscillations in normal motor function as well as their inappropriate expression in other disorders with striatal involvement.

Computational Methods

MSNs. We model MSNs using single-compartment models with Hodgkin-Huxley-type dynamics. Membrane currents (I_{memb}) consist of a fast sodium current (I_{Na}), a fast potassium current (I_{K}), a leak current (I_{L}), and an M-current (I_{M}) (12). We do not model MSN up and down states, which are prevalent during sleep and anesthesia, because these transitions are not prevalent in the awake state (41), which is the focus of our model. Therefore, in our model MSNs, we do not include Kir2 currents, which are active in the MSN down state. The sum of all excitatory input from the cortex and thalamus is modeled using a background excitation term (I_{app}) and Gaussian noise.

Networks. MSNs connect primarily to other MSNs through GABAergic synapses (42). The GABA_A current (I_{GABA}) is modeled using a Hodgkin-Huxley-type conductance with weak GABA_A maximal conductances.

MSNs have extensive local axonal projections that mainly contact other MSNs (42). We construct a striatal model with 100 MSNs and examine several patterns of network connectivity: all-to-all connections, nearest neighbor connections, and 30% random connections, which approximates the rate of connectivity found in both slice and cortex-striatum-substantia nigra organotypic cultures (32, 43).

Parkinsonian Striatum. We model the effect of loss of dopamine indirectly through its effect on ACh-induced reduction of the M-current. Thus, we model the parkinsonian striatum by reducing the maximal M-current conductance from 1.3 to 1.2 mS/cm².

LFP. MSNs account for 90–95% of all neurons in the rat neostriatum (44). LFPs are modeled as the sum of all MSN to MSN GABA_A currents.

Stationarity of the network appears in the raster plots after ~700 ms. To ensure stationarity, our LFP is evaluated only after 1,000 ms of simulated time.

More details are in *SI Computational Methods*.

Experimental Methods

All procedures were done in accordance with the National Institutes of Health Guide for Laboratory Animals and were approved by the Massachusetts Institute of Technology Animal Care and Use and Biosafety Committees. Adult C57 or Swiss Webster mice were used. Under isoflurane anesthesia, a custom-fabricated plastic head plate was surgically affixed to the skull. Adult mice were head-fixed and recorded awake with glass electrodes filled with saline. LFP was collected with a Multiclamp 700B amplifier, digitized with a Digidata 1440 and acquired with pClamp 10 software at a sampling rate of 20 kHz (Molecular Devices). Recordings and infusions in the striatum were made at the stereotactic coordinate (−0.2 to 0.8, 2.0–2.5, 3.0–3.5) that receives projections from both the motor and sensory cortices (45). Infusion in the cortex directly above the striatal infusion sites were at the stereotactic coordinate (−0.2 to 0.8, 2.0–2.5, 1.2–1.7). Carbamoylcholine chloride (Carbachol; from Sigma) was dissolved in saline and infused at a 0.2 $\mu\text{L}/\text{min}$ rate. The infusion cannula was positioned ~300–700 μm away from the recording electrode tip.

The LFP power spectrum was obtained with Hilbert transform in Matlab. More details are in *SI Experimental Methods*.

ACKNOWLEDGMENTS. M.M. and N.K. acknowledge support from National Science Foundation Grant DMS-0717670. E.S.B. acknowledges funding from National Institutes of Health Director's New Innovator Award DP2 OD002002-01. X.H. acknowledges support from the Helen Hay Whitney Foundation Fellowship and National Institutes of Health Grant K99MH085944. N.K. acknowledges support from National Institutes of Health/National Institute of Neurological Disorders and Stroke Grant 1 R01 NS062955-01.

1. DeLong Mahlon R, Juncos Jorge L Parkinson's disease and other extrapyramidal movement disorders. *Harrison's Principles of Internal Medicine* (2008), eds Fauci AS, et al. Available at <http://www.accessmedicine.com/content.aspx?aid=2905868>.
2. Brown P (2007) Abnormal oscillatory synchronisation in the motor system leads to impaired movement. *Curr Opin Neurobiol* 17:656–664.
3. Bevan MD, Magill PJ, Terman D, Bolam JP, Wilson CJ (2002) Move to the rhythm: Oscillations in the subthalamic nucleus-external globus pallidus network. *Trends Neurosci* 25:525–531.
4. Plenz D, Kital ST (1999) A basal ganglia pacemaker formed by the subthalamic nucleus and external globus pallidus. *Nature* 400:677–682.
5. Magill PJ, Bolam JP, Bevan MD (2001) Dopamine regulates the impact of the cerebral cortex on the subthalamic nucleus-globus pallidus network. *Neuroscience* 106:313–330.
6. Yamawaki N, Stanford IM, Hall SD, Woodhall GL (2008) Pharmacologically induced and stimulus evoked rhythmic neuronal oscillatory activity in the primary motor cortex in vitro. *Neuroscience* 151:386–395.
7. Wichmann T, Smith Y, Vitek JL (2002) Pathophysiology of Parkinson's Disease in Chapter 22: Basal ganglia anatomy and physiology. *Parkinson's Disease: Diagnosis and Clinical Management* (online version), eds Factor SA, Weiner WJ (Demos Medical Publishing, New York).
8. Tepper JM, Bolam JP (2004) Functional diversity and specificity of neostriatal interneurons. *Curr Opin Neurobiol* 14:685–692.
9. Kish LJ, Palmer MR, Gerhardt GA (1999) Multiple single-unit recordings in the striatum of freely moving animals: Effects of apomorphine and D-amphetamine in normal and unilateral 6-hydroxydopamine-lesioned rats. *Brain Res* 833:58–70.
10. McCarthy MM, Brown EN, Kopell N (2008) Potential network mechanisms mediating electroencephalographic beta rhythm changes during propofol-induced paradoxical excitation. *J Neurosci* 28:13488–13504.
11. Pervouchine DD, et al. (2006) Low-dimensional maps encoding dynamics in entorhinal cortex and hippocampus. *Neural Comput* 18:2617–2650.
12. Shen W, Hamilton SE, Nathanson NM, Surmeier DJ (2005) Cholinergic suppression of KCNQ channel currents enhances excitability of striatal medium spiny neurons. *J Neurosci* 25:7449–7458.
13. Kreitzer AC (2009) Physiology and pharmacology of striatal neurons. *Annu Rev Neurosci* 32:127–147.
14. Costa RM, et al. (2006) Rapid alterations in corticostriatal ensemble coordination during acute dopamine-dependent motor dysfunction. *Neuron* 52:359–369.
15. DeBoer P, Heeringa MJ, Abercrombie ED (1996) Spontaneous release of acetylcholine in striatum is preferentially regulated by inhibitory dopamine D₂ receptors. *Eur J Pharmacol* 317:257–262.
16. Ikarashi Y, Takahashi A, Ishimaru H, Arai T, Maruyama Y (1997) Regulation of dopamine D₁ and D₂ receptors on striatal acetylcholine release in rats. *Brain Res Bull* 43:107–115.
17. Tseng KY, Kasanetz F, Kargieman L, Riquelme LA, Murer MG (2001) Cortical slow oscillatory activity is reflected in the membrane potential and spike trains of striatal neurons in rats with chronic nigrostriatal lesions. *J Neurosci* 21:6430–6439.
18. Chang JY, Shi LH, Luo F, Woodward DJ (2006) Neural responses in multiple basal ganglia regions following unilateral dopamine depletion in behaving rats performing a treadmill locomotion task. *Exp Brain Res* 172:193–207.
19. Brown P, Williams D (2005) Basal ganglia local field potential activity: Character and functional significance in the human. *Clin Neurophysiol* 116:2510–2519.
20. Mallet N, et al. (2008) Parkinsonian beta oscillations in the external globus pallidus and their relationship with subthalamic nucleus activity. *J Neurosci* 28:14245–14258.
21. Devos D, et al. (2006) Predominance of the contralateral movement-related activity in the subthalamo-cortical loop. *Clin Neurophysiol* 117:2315–2327.
22. Pfurtscheller G, Stancák A, Jr., Neuper C (1996) Post-movement beta synchronization. A correlate of an idling motor area? *Electroencephalogr Clin Neurophysiol* 98:281–293.
23. Sochorova D, Rektor I (2003) Event-related desynchronization/synchronization in the putamen. An EEG case study. *Exp Brain Res* 149:401–404.
24. Koos T, Tepper JM, Wilson CJ (2004) Comparison of IPSCs evoked by spiny and fast-spiking neurons in the neostriatum. *J Neurosci* 24:7916–7922.
25. Bracci E, Panzeri S (2006) Excitatory GABAergic effects in striatal projection neurons. *J Neurophysiol* 95:1285–1290.
26. Tunstall MJ, Oorschot DE, Kean A, Wickens JR (2001) Inhibitory interaction between spiny projection neurons in the rat striatum. *J Neurophysiol* 88:1263–1269.
27. Liang L, DeLong MR, Papa SM (2008) Inversion of dopamine responses in striatal medium spiny neurons and involuntary movements. *J Neurosci* 28:7537–7547.
28. Hardman CD, et al. (2002) Comparison of the basal ganglia in rats, marmosets, macaques, baboons, and humans: Volume and neuronal number for the output, internal relay, and striatal modulating nuclei. *J Comp Neurol* 445:238–255.
29. Stanford IM (2003) Independent neuronal oscillators of the rat globus pallidus. *J Neurophysiol* 89:1713–1717.
30. Chan CS, Shigemoto R, Mercer JN, Surmeier DJ (2004) HCN2 and HCN1 channels govern the regularity of autonomous pacemaking and synaptic resetting in globus pallidus neurons. *J Neurosci* 24:9921–9932.
31. Albin RL, Young AB, Penney JB (1989) The functional anatomy of basal ganglia disorders. *Trends Neurosci* 12:366–375.
32. Taverna S, Ilijic E, Surmeier DJ (2008) Recurrent collateral connections of striatal medium spiny neurons are disrupted in models of Parkinson's disease. *J Neurosci* 28:5504–5512.
33. Koos T, Tepper JM (2002) Dual cholinergic control of fast-spiking interneurons in the neostriatum. *J Neurosci* 22:529–535.
34. Higley MJ, Soler-Llavina GJ, Sabatini BL (2009) Cholinergic modulation of multivesicular release regulates striatal synaptic potency and integration. *Nat Neurosci* 12:1121–1128.
35. Pisani A, Bernardi G, Ding J, Surmeier DJ (2007) Re-emergence of striatal cholinergic interneurons in movement disorders. *Trends Neurosci* 30:545–553.
36. Putzke JD, et al. (2003) Thalamic deep brain stimulation for tremor-predominant Parkinson's disease. *Parkinsonism Relat Disord* 10:81–88.
37. Pfaffinger P (1988) Muscarine and t-LHRH suppress M-current by activating an IAP-insensitive G-protein. *J Neurosci* 8:3343–3353.
38. Terman D, Rubin JE, Yew AC, Wilson CJ (2002) Activity patterns in a model for the subthalamopallidal network of the basal ganglia. *J Neurosci* 22:2963–2976.
39. Roopun AK, et al. (2008) Period concatenation underlies interactions between gamma and beta rhythms in neocortex in vitro. *Front Cell Neurosci*, 10.3389/fnec.03.001.2008.
40. Roopun AK, et al. (2010) Cholinergic neuromodulation controls directed temporal communication in neocortex in vitro. *Front Neural Circuits* 4:8.
41. Mahon S, et al. (2006) Distinct patterns of striatal medium spiny neuron activity during the natural sleep-wake cycle. *J Neurosci* 26:12587–12595.
42. Tepper JM, Wilson CJ, Koos T (2008) Feedforward and feedback inhibition in neostriatal GABAergic spiny neurons. *Brain Res Brain Res Rev* 58:272–281.
43. Czubyko U, Plenz D (2002) Fast synaptic transmission between striatal spiny projection neurons. *Proc Natl Acad Sci USA* 99:15764–15769.
44. Koos T, Tepper JM (1999) Inhibitory control of neostriatal projection neurons by GABAergic interneurons. *Nat Neurosci* 2:467–472.
45. Ramanathan S, Hanley JJ, Deniau JM, Bolam JP (2002) Synaptic convergence of motor and somatosensory cortical afferents onto GABAergic interneurons in the rat striatum. *J Neurosci* 22:8158–8169.